Supporting information for:

Hierarchical Ru-bearing Alumina/Magnetic Iron Oxide Composite for the Magnetically Heated Hydrogenation of Furfural

Sašo Gyergyek*[a], Andraž Kocjan[b], Miha Grilc[c,d], Blaž Likozar[c], Brigita Hočevar[c] and Darko Makovec[a]

[a] Department for Materials Synthesis, Jožef Stefan Institute, Jamova 60, 1000 Ljubljana, Slovenia

E-mail: saso.gyergyek@ijs.si

[b] Department for Nanostructured Materials, Jožef Stefan Institute, Jamova 60, 1000 Ljubljana, Slovenia

[c] Department of Catalysis and Chemical Engineering, National Institute of Chemistry, Hajdrihova 19, 1000 Ljubljana, Slovenia

[d] University of Nova Gorica, Vipavska 13, 5000 Nova Gorica, Slovenia.

1. Experimental details

1.1. Materials

Iron (III) sulphate hydrate ($Fe_2(SO_4)_3 \cdot xH_2O$, Sigma-Aldrich), iron (II) sulphate hydrate ($FeSO_4 \cdot 7H_2O$ 92%, Alfa-Aesar), ammonium hydroxide (NH_4OH 25% solution, J.T. Baker), citric acid monohydrate (ACS 99-102%, Alfa-Aesar), aluminium nitride (AlN, grade C, H.C. Starck), acetone (reagent grade, Carlo-Erba), ruthenium (III) 2,4-pentadionate ($Ru(C_5H_7O_2)_3$ 97%, Sigma-Aldrich), 2-propanol (ACS reagent grade, VWR) were used as received. Furfural (99%, Sigma-Aldrich) was purified by distillation at 20 mbar and 40 °C. As received, furfural is a mild brown liquid (darkened furfural) that over the course of a month severely darkens. Distillation yields colourless liquid that was kept in dark at 4 °C. Initially colourless liquid over the course of a month became lightly yellow and did not visually change over the course of 3 months.

1.2. Magnetic field applicator

An Ambrell (USA) HTG-6000 (6 kW) high-frequency generator was used as an AC current source. A copper-tube coil (Induktio d.o.o., Slovenia) of inner diameter 34 mm, height of 43 mm and 5 turns, resonating at 273 kHz was connected to the generator. The generator and coil were water cooled using closed compressor cooler OBE 003 (2.74 kW).

1.3. Synthesis of catalyst support

Citric-acid-coated iron-oxide nanoparticles MNP-CA were synthesised by the hydrothermal growth of the precipitate at 120 °C, followed by the adsorption of the citrate ion in an aqueous solution using a previously published method [S1,S2]. In brief, 150 ml of ammonium hydroxide was added to the 100 ml of the Fe^{3+} (0.113 mol/L) and Fe^{2+} (0.135 mol/L) in a single rapid pour during vigorous mixing using a magnetic stirrer. The precipitate was transferred to a Teflon-lined stainless steel autoclave and heated for 2h at 120 °C. After cooling naturally, the nanoparticles (MNPs) were washed three times with the dilute ammonium hydroxide solution, having a pH value of 10, using a permanent magnet to separate the MNPs. After the last washing, the MNPs were diluted with DDI water until a final volume of 60 ml. To this slurry, 2.5 ml of citric acid aqueous solution (0.5 g/L) was added and the pH value was set to 5.2 with a diluted solution of ammonium hydroxide. The suspension was heated under reflux and kept at 80 °C for 1.5 h while being constantly stirred with a magnetic stirrer. After cooling naturally, the pH of the suspension was adjusted to the value of 10 using a diluted solution of ammonium hydroxide. MNP-CA nanoparticles were flocculated by the addition of 200 ml of acetone, then separated by a permanent magnet. The liquid part was discarded. The MNP-CA nanoparticles were washed two times using acetone. The MNP-CA were dispersed in 5 ml of DDI water, the suspension was heated to 80 °C for 30 min to remove the residual acetone and centrifuged at 5000 rpm to remove any agglomerates. The concentration of MNPs in the concentrated colloidal aqueous suspension was 161 g/L.

Alumina/magnetic iron oxide composite particles MNP-A were prepared by calcination of a precursor (MNP-B) [S3]. The MNP-B were prepared by hydrolysis of AlN in an aqueous suspension of MNP-CA under reflux conditions [S3]. In a 100-ml round-bottom flask, 39 ml of DDI water was heated to boiling and 1.2 ml of the MNPs suspension was added. When the temperature of the diluted suspension reached 90 °C, 1.23 g of AlN was added and the flask was closed with a reflux condenser. The suspension was left at reflux for 3 h and then left to cool naturally to room temperature. The MNP-B was washed by DDI water four times using a permanent magnet to isolate the particles in between the washing steps. The MNP-B was frozen in liquid nitrogen and freeze-dried overnight. The MNP-B was transformed into MNP-A by calcination for 1 hour at 500 °C in an air atmosphere. MNP-A contained nominally 12 wt.% of MNPs and 88 wt.% of γ-Al_2O_3.

The Ru bearing catalyst MNP-A-Ru was prepared by solvothermal reduction of Ru (III) 2,4-pentadionate in a suspension of MNP-A [S4]. 900 mg of the MNP-A were dispersed in 600 ml of 0.4 mmol/l solution of Ru acetylacetonate in 2-propanol. The suspension was bubbled with Ar gas for 30 min and transferred to a stainless-steel autoclave. The autoclave was sealed and the suspension was heated to 150 ^{o}C under autogenous pressure and kept at 150 ^{o}C for 10 min. After naturally cooling to room temperature the suspension was transferred to a glass beaker and MNP-A-Ru were separated using a permanent magnet. The MNP-A-Ru was washed four times with clean 2-propanol and freeze-dried overnight. Based on the XRF analysis the MNP-A-Ru contained 3.0±0.3 wt.% of Ru.

1.4. Hydrogenation of furfural

0.45 g of the MNP-A-Ru was weighed into the round-bottom glass pressure vessel (Q-Tube-Purging -35-SS, LabTech™), 1.0 g of furfural and 1.1 g of isopropanol were added. The vessel was closed, purged with H_2 gas and pressurized with H_2 to 10 bar.

1.4.1. Conventional heating

The vessel was placed in an oil bath and heated for 1 hour at 90 °C during vigorous stirring (1480 rpm, P=650 W) using a magnetic stirrer. After 1 hour the vessel was left to cool naturally to room temperature. The catalyst was separated using a handheld permanent magnet and the clear liquid part was decanted. The liquid was analysed by GC-QMS (Ultra 2010, Shimadzu, Japan) after dilution with acetone (>99.9% Sigma-Aldrich). The catalyst was washed five times with pure isopropanol and recycled once using the same conditions and loadings.

1.4.2. AC-heating

The vessel was placed in the centre of the inductor coil with the vessel's bottom lifted from the surface of the magnetic stirrer by approx. 1 mm. The field of $\mu_0 H$=30 mT (P=647 W) was turned on during vigorous stirring (1480 rpm) using a magnetic stirrer. The surface temperature of the vessel was continuously monitored using a FLIR™ IR camera. The temperature reached a steady state of 85 °C after 12 min and hydrotreatment was left to proceed for 1 hour. After 1 hour into the reaction the vessel was left to cool naturally to room temperature. The catalyst was separated using a handheld permanent magnet and the clear liquid part was decanted. The liquid was analysed by GC-QMS (Ultra 2010, Shimadzu, Japan) after dilution with acetone (>99.9% Sigma-Aldrich). The catalyst was washed five times with pure isopropanol and recycled four times using the same conditions and loadings.

Stirring the reaction mixture is necessary to achieve the transfer of hydrogen into the liquid phase and to contact the reactants with the catalyst. In our case, a magnetic stirrer was used to achieve the mixing. Magnetic and conductive materials heat in AC fields and therefore the magnetic stirrer and hot plate (used to rotate the stirrer) could also supply heat to the reaction mixture. We conducted an independent experiment to determine to what extent the magnetic stirrer and hotplate contribute to the heating under identical conditions as used for the hydrotreatment. The glass pressure vessel was loaded with 2-propanol and a magnetic stirrer (without MNP-A-Ru catalyst). The vessel was placed in exactly the same positon within the coil as during the hydrotreatment (approx. 1 mm above the surface of the hotplate). The vessel was left open and the fibre optical sensor was used to monitor the temperature of the isopropanol continuously. The stirrer was set to 1480 rpm and the field of $\mu_0 H$=30 mT was turned on. After 30 min the temperature increased by just 5 °C. The experiment proves that the increase of the temperature during the hydrotreatment described above is solely due to heating of MNP-A-Ru under the influence of an AC field.

1.5. Characterization

X-ray powder diffraction patterns (XRD) were collected using a Siemens D5005 diffractometer with a monochromator in the diffracted beam. DIFFRACplus Topas® software was used to estimate the average crystallite size using a fundamental parameters approach to line-profile fitting. A **transmission electron microscope** (TEM) Jeol JEM 2100 operated at 200 kV was used to observe the MNP-CA, MNP-B and MNP-A-Ru particles, deposited on a copper-grid-supported lacy carbon foil. A **scanning-transmission electron microscope** (STEM) Cs-corrected Jeol ARM 200CF STEM operated at 80 kV was used to observe the MNP-A and MNP-A-Ru catalyst, deposited on a copper-grid-supported lacy-carbon foil. During the analysis HAADF and BF detectors were used simultaneously at 68–180 and 10–16 mrad collection semi-angles, respectively. To minimize the specimen drift, images were taken several hours after the insertion of the sample into the microscope and at least 20 minutes after the last sample positioning to minimize the goniometer drift. The chemical composition was analysed using a Jeol Centurio EDXS system with 100 mm^2 SDD. **Nitrogen adsorption/desorption isotherms** were measured for the sample at liquid-nitrogen temperature using a Nova 2000e (Quantachrome) nitrogen-sorption analyser. Prior to the measurement the sample was degassed over night at 120 °C in a vacuum. The surface area was calculated using the Brunauer–Emmett–Teller (BET) equation with nitrogen-adsorption data in the P/P_0 range between 0.05 and 0.3 (7-point analysis), and the pore size distribution, pore volume and average pore size extracted from the desorption branch of the isotherm using the Barrett–Joyner–Halenda (BJH) method. **Room-temperature magnetization curves** of the catalyst MNP-A-Ru as dry powder were measured with a vibrating-sample magnetometer (VSM) LakeShore 7307 VSM. The Ru content in MNP-A-Ru (fresh and spent-after fifth run) was non-destructively determined by using an energy-dispersive **X-ray fluorescence spectrometer (EDXRF)** comprised of a Ge semiconductor detector (GLP-16195/10-P, ORTEC, Oak Ridge, U.S.A) with an energy resolution of 401 eV at 60 keV, a spectroscopy amplifier (M2020, Canberra, Meriden, U.S.A.), ADC (M8075, Canberra, Meriden, U.S.A.) and a PC-based MCA (S-100, Canberra, Meriden, U.S.A.). For the excitation annular Am-241 radioactive source (25 mCi, Isotope Products Laboratories. U.S.A) was used. Quantification was performed utilizing the in-house-developed QAES (Quantitative Analysis of Environmental Samples) software [S5,S6]. For the analysis, sample powders were diluted with cellulose and pressed into a pellet of 24 mm in diameter. Ru surface concentration was determined by **CO pulsed adsorption** using an AutoChem II Chemisorption Analyser (Micrometrics). The sample was first reduced at 473 K for 2 h in stream of 10% H_2 in Ar. Afterwards it was cooled to 273 K in stream of He and pulsed oxidised with O_2. After oxidation, the sample was again reduced and cooled to 273 K in stream of He. At 273 K CO pulses were gradually increased until saturation. The total amount of adsorbed CO was obtained by integration of the peak (saturation). Using the CO: Ru = 1:1 stoichiometry the Ru surface concertation in the nanocatalyst was determined to be 32.5 µmol/g. The **specific absorption rate** (*SAR*) of the MNP-A-Ru was determined from the measurements of the temperature increase in an AC field. 0.25 ml of the suspension of 5 wt.% MNP-A-Ru in isopropanol was placed in a plastic round-bottom 2-ml Eppendorf tube. The tube, which was isolated from the surroundings by a polystyrene chamber, was fitted in the centre of the coil. The temperature at the middle of the sample was continuously measured every second using a fibre-optic probe. The sample was exposed to the AC field for a time varying between 15 s and 20 s. The heating curves were fitted with a linear function in the initial region where the increase in temperature is linear with time. *SAR* values were calculated using the expression:

$$SAR = \frac{c_p}{w}(\frac{\mathrm{d}T}{\mathrm{d}t})_i$$

where c_p is heat capacity of isopropanol (2.68 J/gK), w is the weight fraction of the MNP-A-Ru in isopropanol and $(\mathrm{d}T/\mathrm{d}t)_I$ is slope of the linear fit in the initial region. Relative error of *SAR* was estimated to be 5 % ($\Delta T/T$=2% and $\Delta w/w$=3%).

Size-exclusion chromatography (SEC) was used to characterize neat darkened furfural, distilled furfural and dark-brown distillation residue. The sample was analysed by SEC Size-exclusion chromatographic system (Thermo Scientific Ultimate 3000, ThermoFisher, Waltham, MA, USA) equipped with a RI and UV detector set at 280 nm. The analyses were carried out at the temperature of 30 °C using THF as a mobile phase and for the dilution of samples. The flow rate was set to 1 mL min^{-1}. 100 µL of a diluted (and pre-filtered) sample was injected into Plgel 5 µm MIXED D 7.5 x 300 mm column, which allows the separation by molecular weight up to 400 kDa. The SEC system was previously calibrated with polystyrene standards (in the range of 0.200 – 400 kDa).

Raman spectroscopy was used to determine if coking of the MNP-A-Ru occurred during the hydrotreatment of furfural. The Raman spectrum of the MNP-A-Ru and MNP-A-Ru after fifth recycling (using distilled and neat furfural) of the MN-A-Ru nanocatalyst under AC-field heating was recorded with a NT-MDT model Integra Spectra for Materials Science equipped with a confocal microscope (20x magnification) at room temperature. A 633-nm laser diode was used for the excitation. The scattered light was detected using a cooled CCD camera and a 600 grooves/mm grating.

2. Results and Discussion

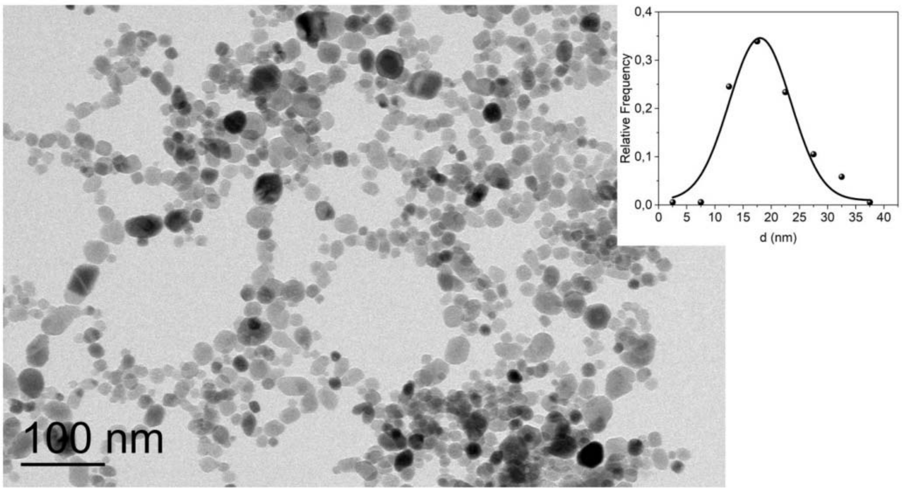

Figure S1. TEM image of the citric-acid-coated magnetic iron-oxide nanoparticles MNP-CA. Inset is the empirical size distribution (circles) and Gaussian fit (curve).

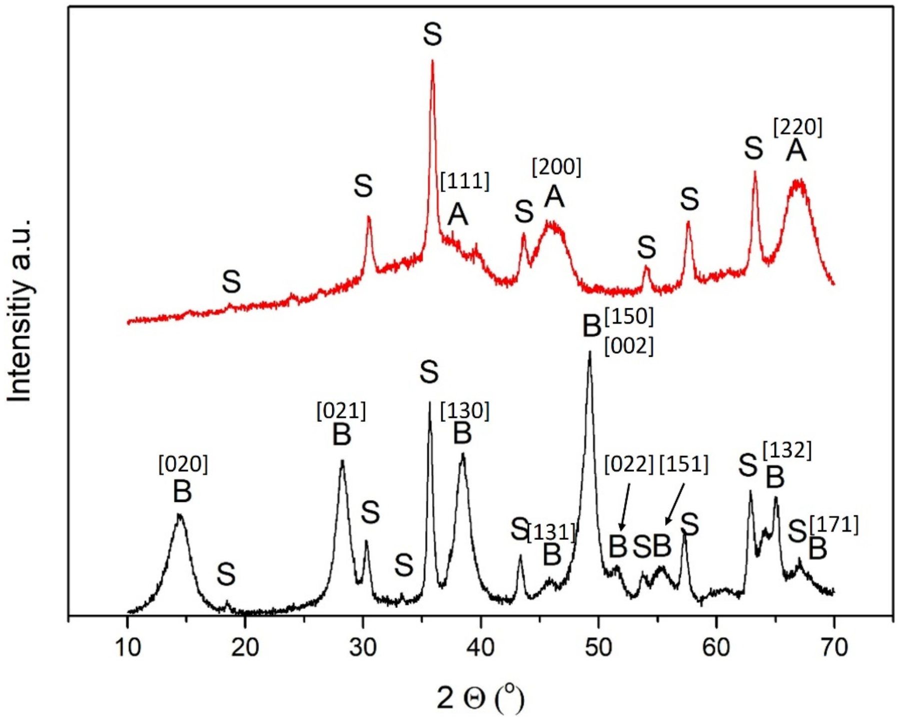

Figure S2. XRD patterns of bohemite/magnetic iron oxide composite precursor MNP-B and alumina/magnetic iron-oxide composite particles MNP-A. S corresponds to the reflections of cubic spinel (iron oxide) (Space group Fd-3m), B to bohemite (orthorhombic Space group Amam) and A to γ-Al_2O_3 (tetragonal I41amd). For clarity only the reflections of bohemite and γ-Al_2O_3 are indexed.

The size of nanocrystallites d_{XRD} was estimated from the XRD peak broadening. The Scherrer equation was used to correlate the peak broadening with the volume-weighted average diameter of the coherently scattering domain, which was interpreted as an average diameter of the crystallites:

S d_{XRD} = 21 nm

B d_{XRD} = 7.0 nm

A d_{XRD} = 3.1 nm

Among iron oxides, only magnetite and maghemite are ferrimagnetic and crystalize in cubic spinel structure [S7]. The structures are closely related and the main difference is that besides Fe^{3+} cations, magnetite contains also Fe^{2+} cations. In maghemite all the Fe^{2+} is oxidized to the Fe^{3+} and the cation vacancies compensate for the oxidation [S7]. The two oxides are miscible and nanoparticles can show a wide range of compositions between magnetite and maghemite. In our previous study [S1] the valence of the Fe cations was determined for the nanoparticles synthesized under identical conditions as the MNPs. The analysis showed the nanoparticles contained only 0.09 of the Fe^{2+} per formula unit. The value of 1 would correspond to the stoichiometric magnetite and a value of 0 to the stoichiometric maghemite. The study also showed that drying the nanoparticles in air at 60 °C resulted in complete oxidation. Considering the very low amount of the Fe^{2+} incorporated in the MNPs and that the MNP-A was prepared by calcination of the MNP-B for 1 hour at 500 ^{o}C in an air atmosphere we can conclude that MNP-A (and MNP-B) contains iron oxide nanoparticles consistent with maghemite structure.

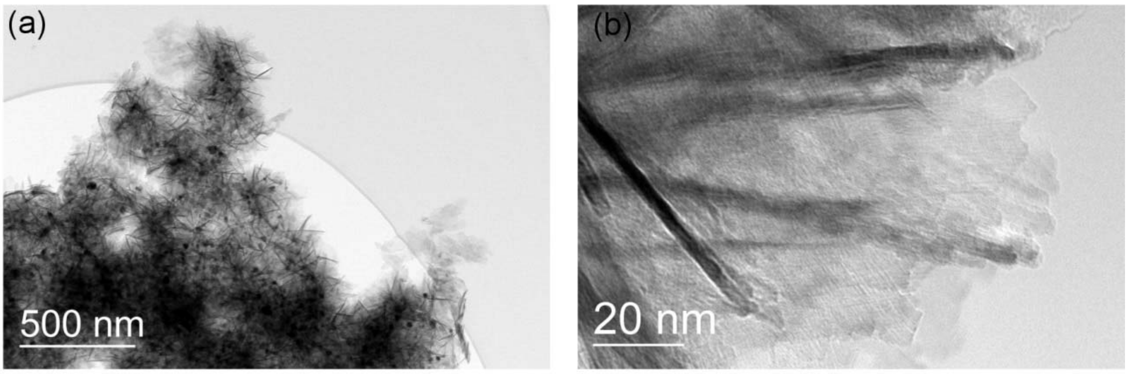

Figure S3. TEM image of bohemite/magnetic iron oxide composite precursor MNP-B at lower (a) and higher (b) magnification.

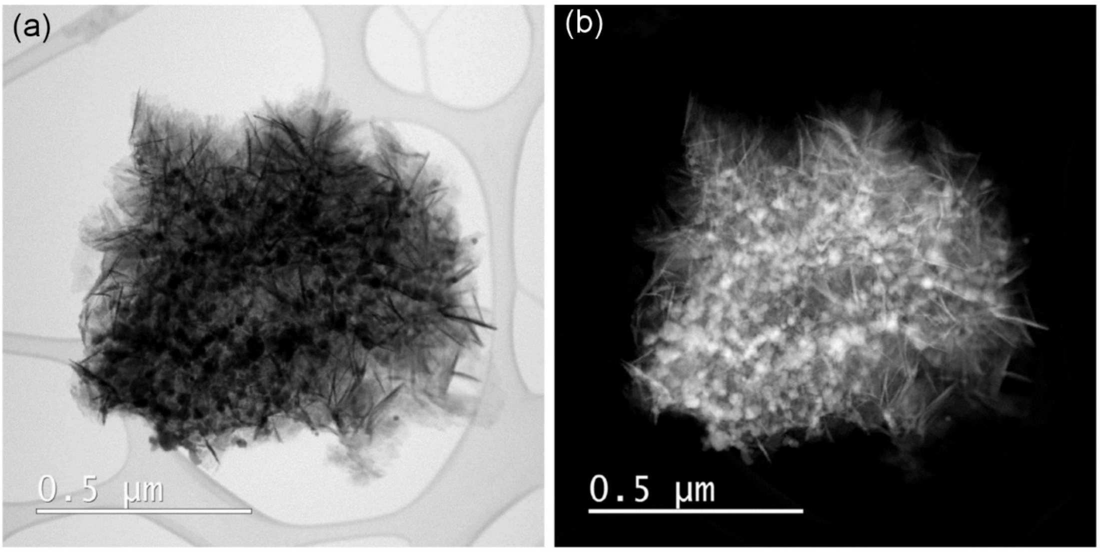

Figure S4. BF (a) and HAADF (b) STEM images of alumina/magnetic iron oxide composite particles MNP-A.

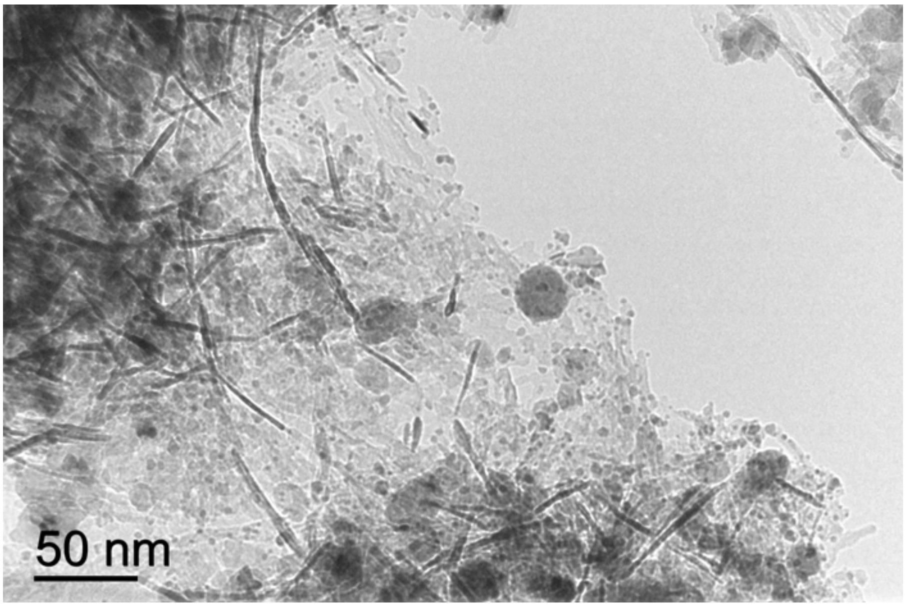

Figure S5: TEM image of the catalyst MNP-A-Ru.

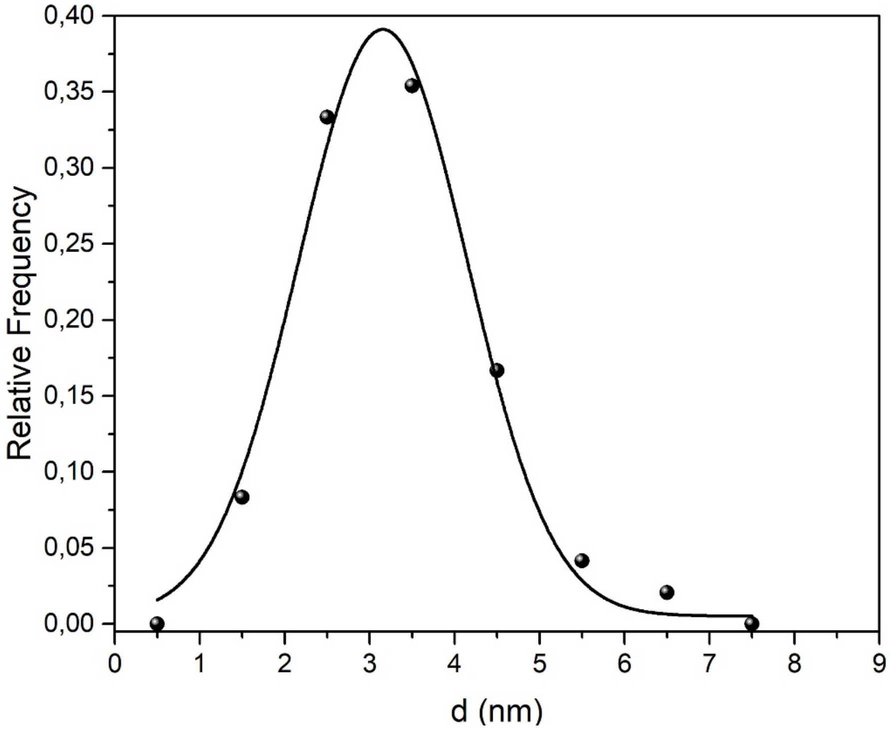

Figure S6. Number-weighted empirical size distribution (dots) of the Ru nanoparticles in the MNP-A-Ru and Gaussian fit (curve).

The empirical size distribution was estimated by measuring area of the Ru nanoparticles on the TEM image. The particle size d_{TEM} is given as an equivalent diameter—the diameter of a circle having the same surface area as the imaged particle.

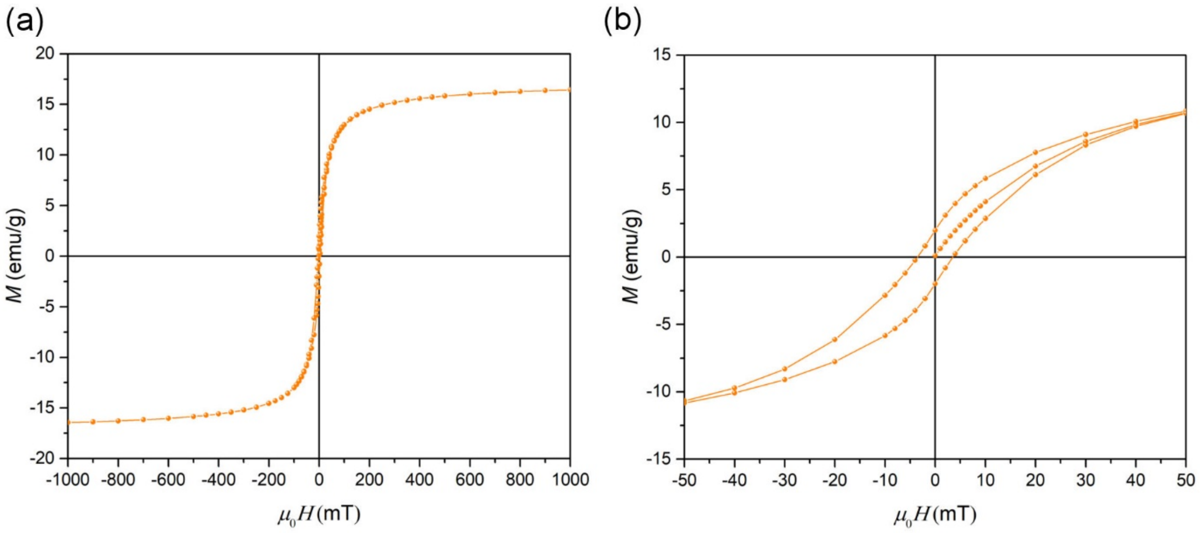

Figure S7. Room-temperature magnetization curve of the catalyst MNP-A-Ru (a) and enlargement of the low-field area (b).

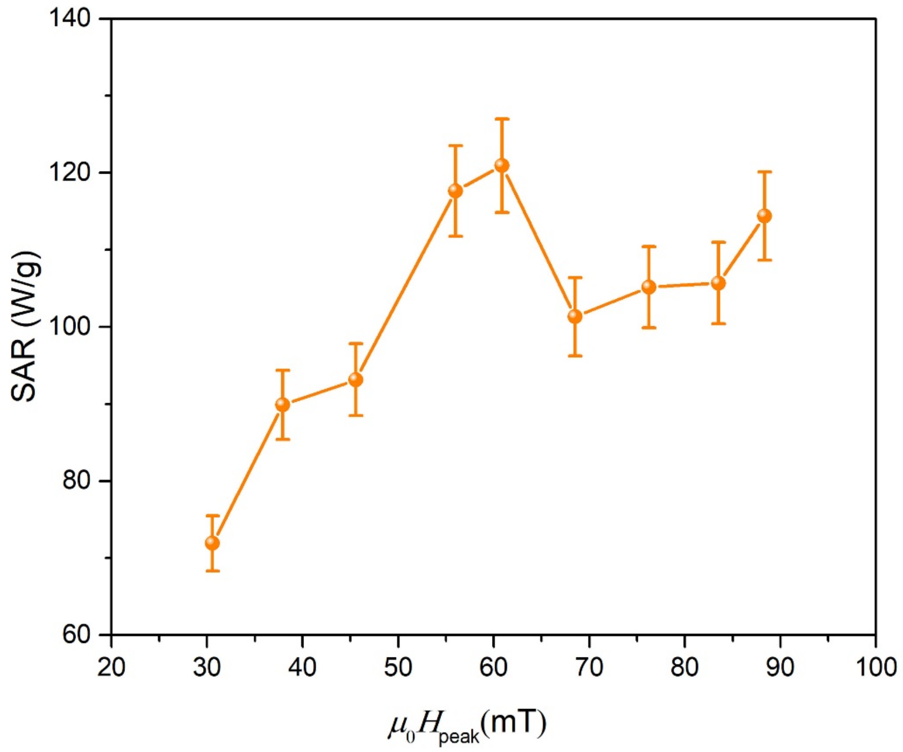

Figure S8. SAR of the MNP-A-Ru as a function of the AC-field amplitude.

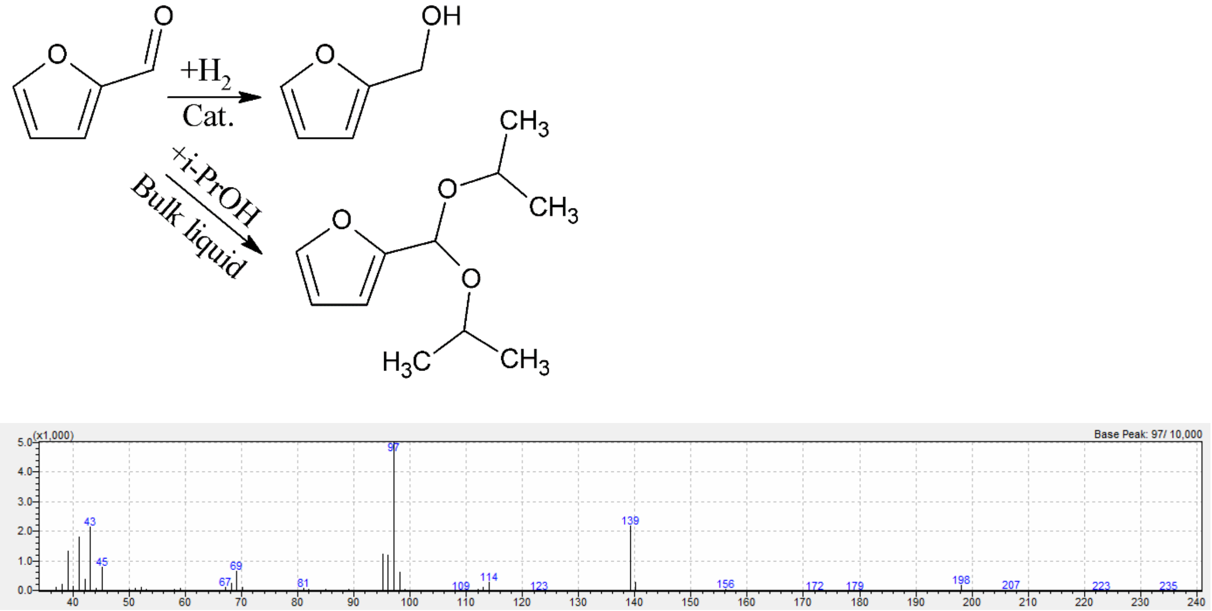

Figure S9. Reaction pathways and mass spectrum of diisopropyl acetal.

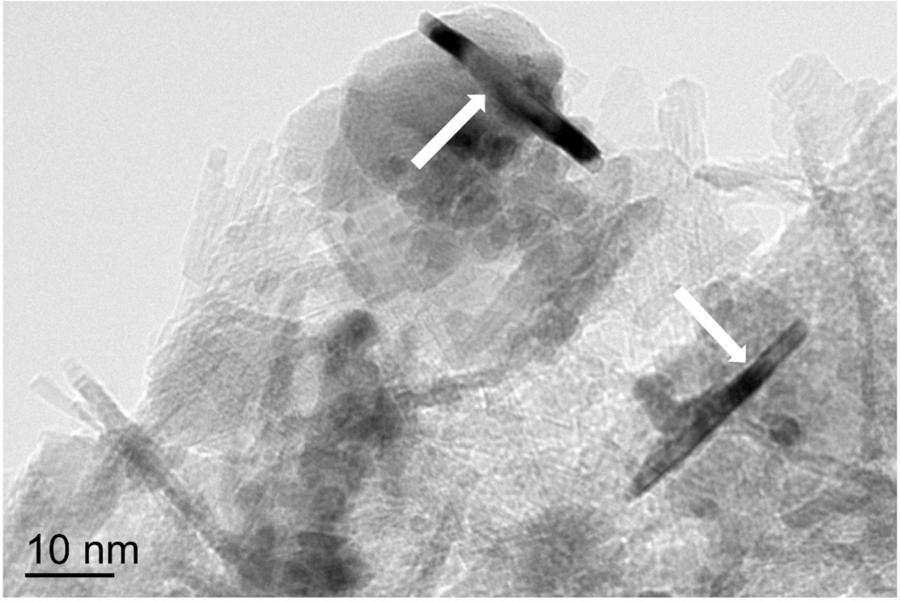

Figure S10. TEM image of the spent MNP-A-Ru (after fifth recycle under AC-field heating). Ru nanoplatelets are marked with arrows.

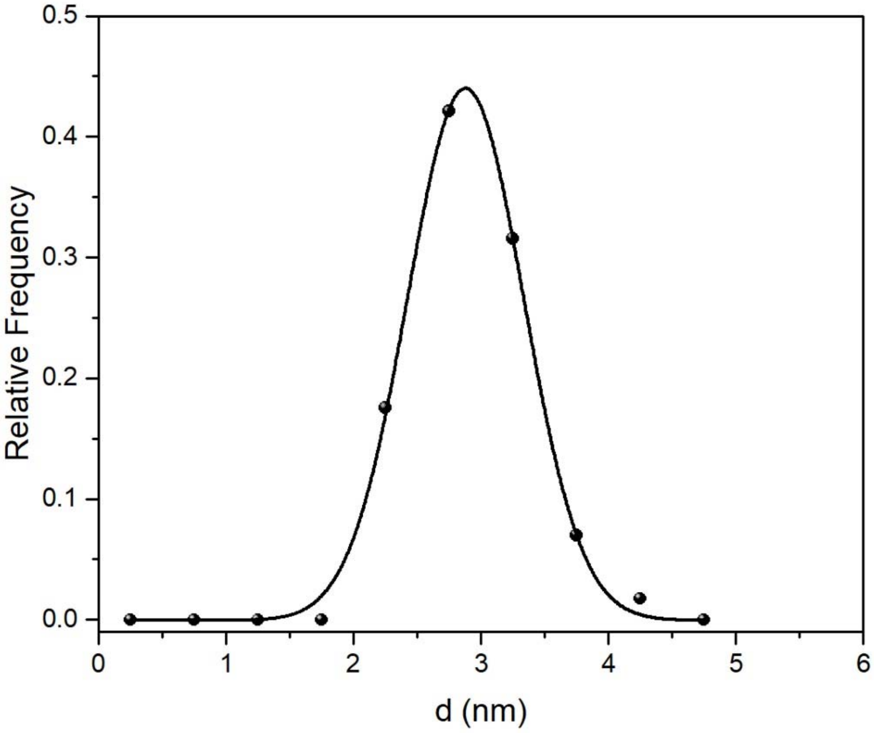

Figure S11. Number-weighted empirical size distribution (dots) of the Ru nanoparticles in the spent MNP-A-Ru and Gaussian fit (curve).

Furfural was eluted from the SEC column at the RT of 31 min, while two small peaks representing polymerized furfural can be clearly seen at the RT 29 and 30 min when aged furfural and distillation residue were injected. The presence of polymerized compounds was not detected in the case of distilled furfural.

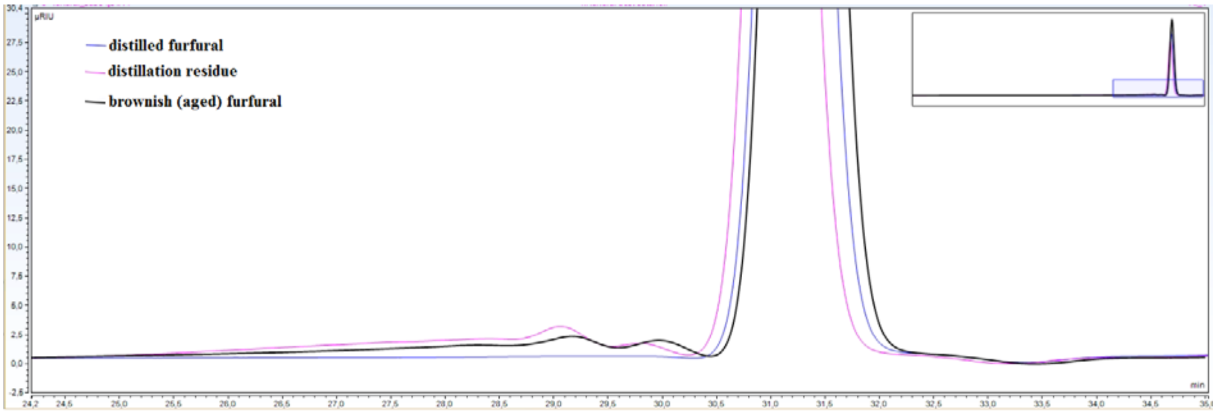

Figure S12. SEC chromatograms of the distilled furfural, distillation residue and dark-brown aged furfural.

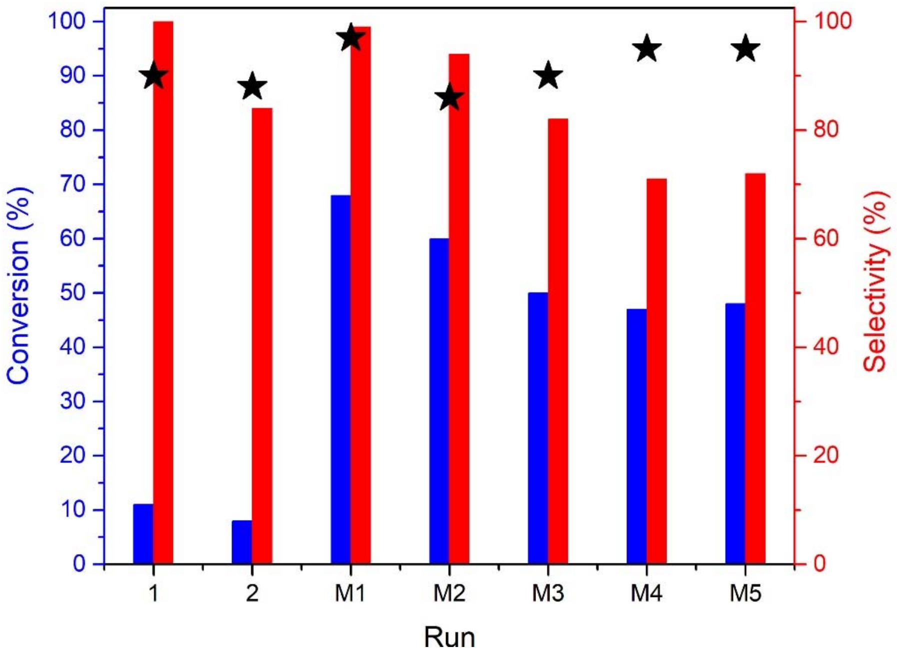

Figure S13. Recycling of the MN-A-Ru catalyst under conventional heating (Runs 1 and 2) and under AC-filed heating (Runs M1 and M5) using neat furfural. Stars represent C balance. Reaction conditions: MNP-A-Ru (0.45 g), neat furfural (1.0 g, 10.4 mmol), 2-propanol (11 g), H_2 1 MPa, 90 °C, 1 h.

References

[S1] S. Gyergyek, D. Makovec, M. Jagodič, M. Drofenik, K. Schenk, O. Jordan, J. Kovač, G. Dražič, H. Hofmann, *J. Alloys Compd*. **2017**, *694*, 261-271.

[S2] S. Campelj, D. Makovec and M. Drofenik, *J. Phys. Condens. Matter*, 2008, **20**, 204101.

[S3] S. Gyergyek, A. Kocjan, D. Makovec, United Kingdom (GB) Patent Application No: GB1903020.4.

[S4] S. Gyergyek, A. Kocjan, A. Bjelić, M. Grilc, B. Likozar, D. Makovec, *Mater. Res. Lett*. 2018, 6, 426-431.

[S5] M. Nečemer, P. Kump, K. Vogel-Mikuš, *Handbook of Phytoremediation* (Ed. I.A., Golubev), 2011, Nova Science Publishers, New York.

[S6] M. Nečemer, P. Kump, J. Ščančar, R. Jaćimović, J. Simčič, P. Pelicon, M. Budnar, Z. Jeran, P. Pongrac, M. Regvar, K. Vogel-Mikuš, 2008, *Spectrochim. Acta Part B*, 2008, **63**, 1240-1247.

[S7] R. M. Cornell, U. Schwertmann, *The Iron oxides (2nd Ed.)*, Wiley-VCH, Weinheim, **2000**. pp. 32-34 and pp. 365-368.